Tuning Conductance in π−σ−π Single-Molecule Wires

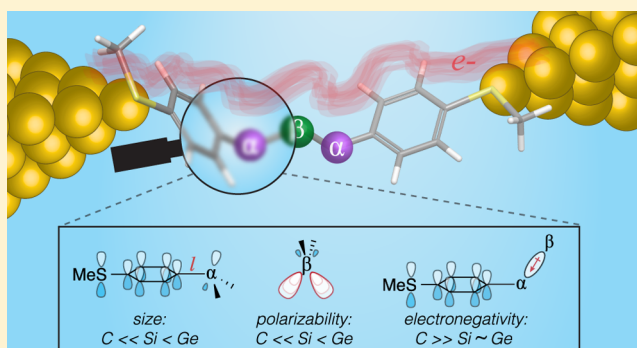Timothy A. Su,[†,§] Haixing Li,[‡,§] Rebekka S. Klausen,[†,⊥] Jonathan R. Widawsky,[‡] Arunabh Batra,[‡] Michael L. Steigerwald,*[†] Latha Venkataraman,*[†,‡] and Colin Nuckolls*[†]

[†]Department of Chemistry, Columbia University, New York, New York 10027, United States
[‡]Department of Physics and Applied Math, Columbia University, New York, New York 10027, United States

ⓢ *Supporting Information*

ABSTRACT: While the single-molecule conductance properties of π-conjugated and σ-conjugated systems have been well-studied, little is known regarding the conductance properties of mixed σ−π backbone wires and the factors that control their transport properties. Here we utilize a scanning tunneling microscope-based break-junction technique to study a series of molecular wires with π−σ−π backbone structures, where the π-moiety is an electrode-binding thioanisole ring and the σ-moiety is a triatomic α−β−α chain composed of C, Si, or Ge atoms. We find that the sequence and composition of group 14 atoms in the α−β−α chain dictates whether electronic communication between the aryl rings is enhanced or suppressed. Placing heavy atoms at the α-position decreases conductance, whereas placing them at the β-position increases conductance: for example, the C−Ge−C sequence is over 20 times more conductive than the Ge−C−Ge sequence. Density functional theory calculations reveal that these conductance trends arise from periodic trends (i.e., atomic size, polarizability, and electronegativity) that differ from C to Si to Ge. The periodic trends that control molecular conductance here are the same ones that give rise to the α and β silicon effects from physical organic chemistry. These findings outline a new molecular design concept for tuning conductance in single-molecule electrical devices.

INTRODUCTION

In this study we systematically vary the strength of coupling between the π and σ backbone components of a molecular wire to raise or lower the conductance of a single-molecule electrical device. The miniaturization of electronic devices and the related interest in creating molecular-scale devices have motivated the desire to understand the charge transport characteristics of molecules. There have been many studies that have elucidated how the strength of σ-conjugation or π-conjugation within a molecular wire backbone can be tuned to control single-molecule conductance.[1−6] Ottosson and coworkers have studied σ−π conjugation computationally and spectroscopically.[7] However, there has yet to be an experimental description of how the coupling between σ and π backbone components influences molecular conductance. Though organic electronic materials commonly feature π−σ substructures,[8−12] it is not well understood how the nature of the π−σ interaction affects charge transport.

For this study we create a test bed of molecular wires with π−σ−π backbone structures, where the π-substructure is an electrode-binding p-thioanisole ring and the σ-moiety is a triatomic α−β−α sequence of catenated group 14 atoms (α and β = C, Si, or Ge) (Figure 1). We systematically vary the composition and sequence of atoms in the σ-chain to understand how such alterations influence conductance. We
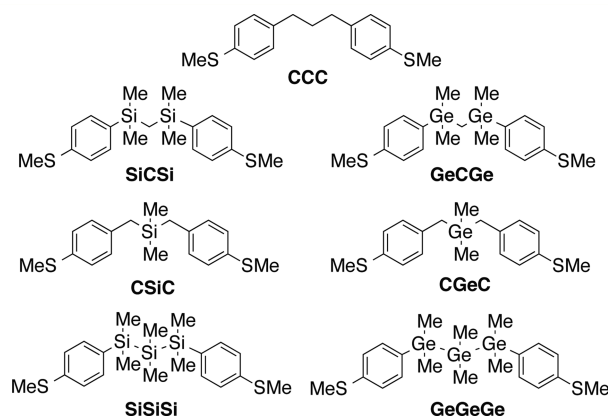

Figure 1. Chemical structures of the π−σ−π molecular wires.

see two counterbalancing trends in the data. Conductance decreases as the α atom is varied from C to Si to Ge; however, conductance increases as the composition of the β atom changes from C to Si to Ge. Mechanistic chemical analysis and density functional theory (DFT) calculations suggest that these opposing conductance trends arise from differences in how the

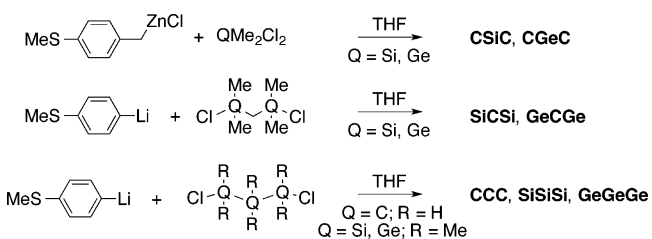atomic composition and sequence within the $\alpha-\beta-\alpha$ chain influence the coupling between the σ-chain and the thioanisole ring. These effects are the single-molecule conductance equivalent of the α silicon and β silicon hyperconjugation that is an essential component of physical organic chemistry. Hyperconjugation provides an intellectual bridge between physical organic chemistry and the conductance trends we observe here.

■ RESULTS AND DISCUSSION

Synthesis. We synthesize **CSiC** and **CGeC** from the double addition of 4-(methylthio)benzylzinc chloride[13] to dimethyl-dichlorosilane or dimethyldichlorogermane (Scheme 1). We

Scheme 1. Synthesis of the $\alpha-\beta-\alpha$ Wires with p-Thioanisole End Groups

MeS——CH₂ZnCl + QMe₂Cl₂ →(THF, Q = Si, Ge)→ **CSiC, CGeC**

MeS——Li + Cl-Q~Q-Cl (Me Me / Me Me) →(THF, Q = Si, Ge)→ **SiCSi, GeCGe**

MeS——Li + Cl-Q~Q~Q-Cl (R R R / R R R) →(THF, Q = C; R = H / Q = Si, Ge; R = Me)→ **CCC, SiSiSi, GeGeGe**

prepared **SiCSi**, **GeCGe**, **CCC**, **SiSiSi**, and **GeGeGe** by reacting 4-(methylthio)phenyllithium with the appropriate halide-terminated σ-chain.[2,14−16] The Supporting Information (SI) contains further details for the preparation and characterization of these molecular wires.

STM-BJ Measurement Details. We measure the conductance of these molecules with a scanning tunneling microscope-based break-junction (STM-BJ) technique.[1] In this technique, Au−molecule−Au junctions are measured by repeatedly breaking and forming point contacts between the Au tip and substrate in a solution of the target molecule in 1,2,4-trichlorobenzene under ambient conditions. After the Au−Au point contact is broken, the aurophilic thiomethyl groups on the molecule bind the electrodes to form a Au−molecule−Au junction. Conductance is measured across the junction as a function of tip−substrate displacement, and the resulting measurement traces reveal molecule-dependent plateaus signifying junction formation with conductance values below G_0 ($2e^2/h$), the quantum of conductance describing a single Au−Au atomic contact.[17] The junction breaks once the distance between the electrodes becomes too large for the molecule to span. We form and break thousands of molecular junctions and analyze all measured traces using logarithmically-binned one-dimensional (1D) histograms[18] that provide a distribution of measured conductance values for all traces.

Single-Molecule Conductance Data Analysis. The 1D conductance histograms for the $\alpha-\beta-\alpha$ wires are shown in Figure 2. Table 1 lists the conductance peak values for the molecules measured here. The purple rows in Table 1 demonstrate that varying the α-position from C to Si to Ge (while fixing the β-atom as C) results in a conductance trend that follows **GeCGe < SiCSi < CCC**. Conversely, the blue rows in Table 1 show that varying the β-position from C to Si to Ge (while fixing the α-atom as C) increases conductance such that **CCC < CSiC < CGeC**. To highlight these competing trends, the conductance of **CGeC** is over 20 times that of **GeCGe**. These opposing trends negate each other when both the α- and
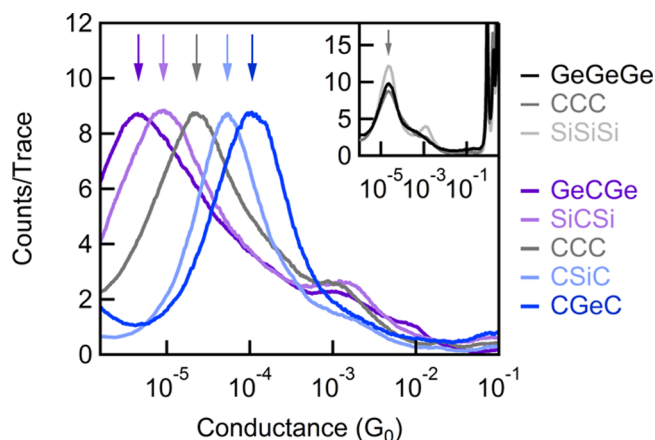

Figure 2. Logarithmically-binned 1D conductance histograms of **GeCGe**, **SiCSi**, **CCC**, **CSiC**, and **CGeC**. The 1D histograms compile over 10 000 measurement traces without data selection for each molecule. Conductance peak maxima (marked by arrows) are obtained from Gaussian fits to the conductance data. The counts/trace intensities of these conductance peaks are normalized by factors of 0.88, 1.15, 1.00, 0.70, and 0.82 respectively to highlight conductance trends. The unscaled conductance histograms of **CCC**, **SiSiSi**, and **GeGeGe** are shown in the inset; these molecules have approximately the same conductance. We observe a small conductance peak at ~10⁻³ G_0 that we have discussed previously;[19,20] it is due to an interaction between the Au electrodes and $\alpha-\beta$ σ-bond (see SI for additional comments).

Table 1. Conductance Values from STM-BJ Measurements, DFT-Calculated Orbital Energies, and DFT-Calculated Molecular Lengths

	Cond.[a] (×10⁻⁶ G₀)	HOMO[b] (eV)	HOMO-1[b] (eV)	Splitting[c] (eV)	σ-Chain Length[d] (Å)
GeCGe	4.7	−5.74	−5.83	0.09	6.4 (+1.3)
SiCSi	9.1	−5.74	−5.84	0.10	6.1 (+1.0)
CCC	23.1	−5.64	−5.78	0.14	5.1 (0)
CSiC	53.5	−5.51	−5.68	0.17	5.7 (+0.6)
CGeC	108	−5.46	−5.68	0.22	5.8 (+0.7)
SiSiSi	23.8	−5.63	−5.84	0.21	6.9 (+1.8)
GeGeGe	22.1	−5.60	−5.81	0.21	7.3 (+2.2)

[a]Conductance peak value obtained from fitting a Gaussian curve to the corresponding 1D conductance histogram. [b]Calculated at the B3LYP/cc-pVTZ level of DFT. [c]Difference in energy between the antisymmetric and symmetric combinations of the S pπ lone pairs (the HOMO and HOMO−1 respectively). [d]Through-space distance between the aryl carbons that terminate the $\alpha-\beta-\alpha$ chain in the DFT optimized structure. The length relative to **CCC** is given in parentheses.

β-positions are varied (gray rows in Table 1): the **CCC**, **SiSiSi**, and **GeGeGe** $\pi-\sigma-\pi$ wires give approximately the same conductance value.

The conductance trends we observe are related to the particular composition and sequence of group 14 atoms in the $\alpha-\beta-\alpha$ chain that dictate the extent to which the aryl rings interact with one another through the bridging σ-chain. Changing the composition of the α and β atoms modulates three major electronic factors within the molecule (Figure 3A−C).
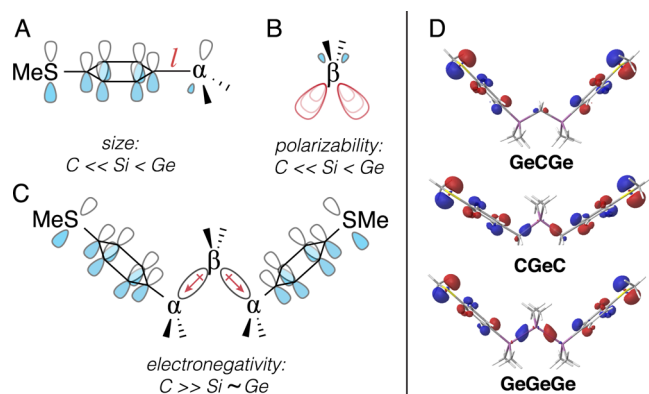
Figure 3. (A–C) Atomic size, polarizability, and electronegativity dictate the strength of interaction between the thioanisole rings through the σ-chain and, thereby, the conductance of the wire. (D) The influence of three periodic factors on the nature of the $\pi-\sigma$ interaction is apparent in the HOMO surfaces (isovalue = 0.05) for **GeCGe**, **CGeC**, and **GeGeGe**. These structures were calculated at the B3LYP/cc-PVTZ level.

The first factor is specific to the α atom (Figure 3A): the Ar–C bond length (1.51 Å) is substantially shorter than the Ar–Si (1.89 Å) and Ar–Ge (1.98 Å) bond lengths.[21] As a result, the aryl ring and σ-chain interact more strongly when α = C than when α = Si or Ge because the ring is brought into closer proximity to the central σ-chain. The second factor (Figure 3B), atomic polarizability, follows the trend C $\ll$ Si < Ge.[22] Atomic polarizability dictates the electron donating ability and diffuseness of the $\alpha-\beta$ σ-bond and thereby influences the ability of the σ-bond to electronically interact with the thioanisole π-orbitals. The third factor (Figure 3C) arises from the polarity of the $\alpha-\beta$ bond. The electron density of a C–Si or a C–Ge σ-bond is directed toward the C atom rather than the Si or Ge atom because C is much more electronegative than Si or Ge.[23] The $\alpha-\beta$ bond polarity is an important factor because it dictates whether the σ-bond electron density is oriented toward the aryl ring or away from it.

Based on these three factors, the CH_2–$GeMe_2$ σ-bonds in **CGeC** interact more strongly with the thioanisole π-orbitals than they do in **GeCGe**. The shorter Ar–C bond brings the aryl ring and σ-chain into closer contact for **CGeC** than the Ar–Ge bond does for **GeCGe**. Furthermore, the $\alpha-\beta$ bond density is polarized toward the aryl rings in **CGeC**, but away from the aryl rings in **GeCGe**. The characteristics of **GeGeGe** balance the three factors described above: the Ar–Ge bond is relatively long, but the Ge–Ge $\alpha-\beta$ bond is more polarizable and more covalent (the electron density is spread more evenly between the two atom centers) than in the Ge–C bonds.

Density Functional Theory Analysis. DFT calculations provide a numerical assessment of how these three chemical features influence the molecule's electronic properties (see the Supporting Information for notes and details of the calculations).[24] Conductance across a molecular junction is facilitated by two primary molecular factors: (1) close energetic alignment between the conducting orbital of the molecule and the Fermi level (E_F) of the electrode and (2) strong coupling between the two distal lone pair orbitals that link the molecule to the electrodes.[25–27] As we have shown previously, it is particularly informative to investigate the highest energy molecular orbitals that describe the lone pair orbitals.[19,27] In the case of the molecules studied here, these molecular orbitals

are the HOMO and HOMO−1 that comprise the antisymmetric ($S_1 − S_2$) and symmetric ($S_1 + S_2$) combinations of the two S $p\pi$ lone pairs, respectively.

Conductance should increase as the $S_1 − S_2$ orbital rises in energy and is brought into closer alignment with the Fermi energy (E_F). Conductance should also increase as the communication between the S $p\pi$ lone pairs becomes stronger. We can assess the coupling between the lone pairs by comparing the difference in energy between the $S_1 − S_2$ and $S_1 + S_2$ molecular orbitals: a small splitting indicates that the lone pairs are mostly independent and noninteracting, whereas a large splitting indicates that the lone pairs are strongly coupled.[19] We can therefore estimate the conductive impact of tuning the α and β atom composition by evaluating two parameters from our DFT calculations: the $S_1 − S_2$ (HOMO) energy and the energy difference between the antisymmetric and symmetric combinations of the S $p\pi$ orbitals (HOMO/HOMO−1 splitting). We list the values of the energies for these two orbitals in Table 1.

The DFT trends are consistent with the chemical analysis described above. The interaction of the $\alpha-\beta$ σ-bonds with the thioanisole π-orbitals is visually apparent in the HOMO surfaces in Figure 3D. From **CCC** to **SiCSi** to **GeCGe**, the HOMO becomes lower in energy and the splitting magnitude decreases because the electron density of the $\alpha-\beta$ bond is removed further away from the thioanisole rings. The HOMO rises in energy, and the HOMO/HOMO−1 splitting becomes larger going from **CCC** to **CSiC** to **CGeC** due to the C–Si(Ge) bond polarity and the increasing donor power of the β atom. The HOMO value of **CCC** is similar to that of **SiSiSi** and **GeGeGe**: though the C–C σ-bond is less donating than the Si–Si or Ge–Ge bond, it still strongly destabilizes the thioanisole π-orbitals because of the shorter Ar–C bond. The smaller HOMO/HOMO−1 splitting calculated for **CCC** is consistent with the weaker conjugation of C–C σ-bonds compared to Si–Si and Ge–Ge σ-bonds.[14]

Analogy to α and β Silicon Hyperconjugation Effects. The periodic trends that control conductance here are the same ones that form the basis of the α and β silicon effects, which are fundamental principles of hyperconjugation from physical organic chemistry.[28,29] This is shown schematically in Figure 4A. These effects describe the electronic interaction between a π orbital and an adjacent C–Si σ-bond based on whether the Si atom is either one atom (α) or two atoms (β) away from the π orbital. For example, carbocations are weakly stabilized by α-Si atoms[30] but are strongly stabilized by β-Si atoms.[31] The conductance trends we observe here are thus an electrical manifestation of the α and β silicon effects.

A well-established metric for gauging the strength of hyperconjugation is the Hammett parameter, σ_p^+, which indexes the extent to which a positive charge on a benzene ring is stabilized by a particular substituent.[32] Negative values for σ_p^+ correspond to stronger electron donation from the substituent to the phenyl ring. Previously, we demonstrated a correlation between the logarithmic conductance ratio and Hammett parameter for electron-donating and -withdrawing substituents on 1,4-diaminobenzene.[33] In Figure 4B we apply a similar approach in comparing $\log(G_{\alpha-\beta-\alpha}/G_{CCC})$ against the σ_p^+ value for structurally similar molecules from ref 34, given here in parentheses: **GeCGe** ($PhGeMe_3$), **SiCSi** ($PhSiMe_3$), **CCC** ($PhCH_2Me$), **CSiC** ($PhCH_2SiMe_3$), and **CGeC** ($PhCH_2GeMe_3$). Such analysis reveals an approximately linear agreement.
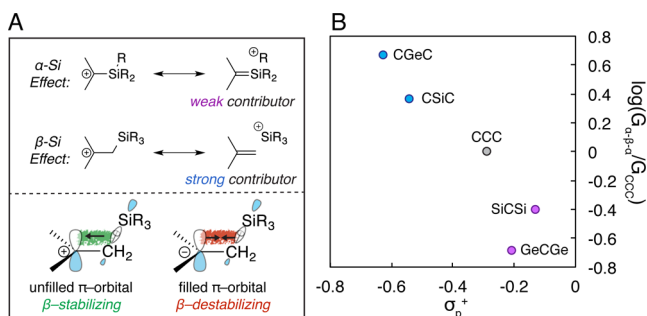
Figure 4. (A) Common representations of the β silicon effect in physical organic chemistry. The top panel describes the resonance pictures of the α- and β-stabilizing silicon effects. The bottom panel juxtaposes the β-stabilizing effect with the β-destabilizing effect; the β-destabilizing picture is relevant to the HOMO energy trends observed in the $\pi-\sigma-\pi$ wires. (B) The logarithm of the $\pi-\sigma-\pi$ wire's conductance relative to that of **CCC** is plotted against the Hammett σ_p^+ coefficients (relative to benzene) obtained for molecules from ref 34 that are similar in structure to the ones studied here.

Despite the fact that the Hammett experiments do not fully replicate the break-junction environment, this simple approach correlates quite well with the observed conductance trends. The general correlation we find between conductance and σ_p^+ supports the idea that tailoring the strength of $\sigma-\pi$ interactions is useful not only for altering chemical reaction rates but also for tuning charge transport in single-molecule junctions.

■ CONCLUSIONS

The observed conductance trends, chemical analysis, and DFT calculations reveal two new design rules for $\pi-\sigma-\pi$ wires that ultimately arise from periodic trends such as atomic size, polarizability, and electronegativity: (1) placing heavy atoms (Si, Ge) in the α-position of the σ-chain decreases the conductance of the wire by diminishing the interaction between the thioanisole rings, and (2) placing heavy atoms in the β-position increases junction conductance by providing a stronger electronic pathway for communication between the aryl rings. These design principles can extend to bulk electronic materials as well: one possible opportunity is to simultaneously solubilize and tune the electronics of π-conjugated polymers by replacing the β-carbon atom of an alkyl solubilizing chain with a silicon or germanium atom. More broadly, our results demonstrate that the principles of physical organic chemistry are an untapped vein[27] for designing molecules and tuning charge transport for single-molecule electronics.

■ ASSOCIATED CONTENT

ⓢ Supporting Information

The Supporting Information is available free of charge on the ACS Publications website at DOI: 10.1021/jacs.6b04394.

> Additional comments, synthetic procedures, characterization of compounds, STM-BJ measurement details, and computational details (PDF)

■ AUTHOR INFORMATION

Corresponding Authors

*mls2064@columbia.edu
*lv2117@columbia.edu
*cn37@columbia.edu

Present Address

⊥Department of Chemistry, The Johns Hopkins University, Baltimore, MD 21218, USA.

Author Contributions

§T.A.S. and H.L. contributed equally.

Notes

The authors declare no competing financial interest.

■ ACKNOWLEDGMENTS

■ REFERENCES

(1) Xu, B.; Tao, N. J. *Science* **2003**, *301*, 1221.
(2) Klausen, R. S.; Widawsky, J. R.; Steigerwald, M. L.; Venkataraman, L.; Nuckolls, C. *J. Am. Chem. Soc.* **2012**, *134*, 4541.
(3) Su, T. A.; Li, H.; Steigerwald, M. L.; Venkataraman, L.; Nuckolls, C. *Nat. Chem.* **2015**, *7*, 215.
(4) Mayor, M.; Weber, H. B.; Reichert, J.; Elbing, M.; von Hänisch, C.; Beckmann, D.; Fischer, M. *Angew. Chem., Int. Ed.* **2003**, *42*, 5834.
(5) He, J.; Chen, F.; Li, J.; Sankey, O. F.; Terazono, Y.; Herrero, C.; Gust, D.; Moore, T. A.; Moore, A. L.; Lindsay, S. M. *J. Am. Chem. Soc.* **2005**, *127*, 1384.
(6) Venkataraman, L.; Klare, J. E.; Nuckolls, C.; Hybertsen, M. S.; Steigerwald, M. L. *Nature* **2006**, *442*, 904.
(7) (a) Emanuelsson, R.; Löfås, H.; Zhu, J.; Ahuja, R.; Grigoriev, A.; Ottosson, H. *J. Phys. Chem. C* **2014**, *118*, 5637. (b) Emanuelsson, R.; Denisova, A. V.; Baumgartner, J.; Ottosson, H. *Organometallics* **2014**, *33*, 2997. (c) Göransson, E.; Emanuelsson, R.; Jorner, K.; Markle, T. F.; Hammarström, L.; Ottosson, H. *Chem. Sci.* **2013**, *4*, 3522.
(8) Miller, R. D.; Michl, J. *Chem. Rev.* **1989**, *89*, 1359.
(9) Chicart, P.; Corriu, R. J. P.; Moreau, J. J. E.; Garnier, F.; Yassar, A. *Chem. Mater.* **1991**, *3*, 8.
(10) Usta, H.; Lu, G.; Facchetti, A.; Marks, T. J. *J. Am. Chem. Soc.* **2006**, *128*, 9034.
(11) Sun, Y.; Welch, G. C.; Leong, W. L.; Takacs, C. J.; Bazan, G. C.; Heeger, A. J. *Nat. Mater.* **2011**, *11*, 44.
(12) Surampudi, S.; Yeh, M.-L.; Siegler, M. A.; Hardigree, J. F. M.; Kasl, T. A.; Katz, H. E.; Klausen, R. S. *Chem. Sci.* **2015**, *6*, 1905.
(13) Metzger, A.; Piller, F. M.; Knochel, P. *Chem. Commun.* **2008**, 5824.
(14) Su, T. A.; Li, H.; Zhang, V.; Neupane, M.; Batra, A.; Klausen, R. S.; Kumar, B.; Steigerwald, M. L.; Venkataraman, L.; Nuckolls, C. *J. Am. Chem. Soc.* **2015**, *137*, 12400.
(15) Barrau, J.; Hamida, N. B.; Satge, J. *J. Organomet. Chem.* **1985**, *282*, 315.
(16) Barton, T. J.; Hoekman, S. K. *J. Am. Chem. Soc.* **1980**, *102*, 1584.
(17) Agraït, N.; Rodrigo, J.; Vieira, S. *Phys. Rev. B: Condens. Matter Mater. Phys.* **1993**, *47*, 12345.
(18) Gonzalez, M. T.; Wu, S.; Huber, R.; van der Molen, S. J.; Schönenberger, C.; Calame, M. *Nano Lett.* **2006**, *6*, 2238.
(19) Klausen, R. S.; Widawsky, J. R.; Su, T. A.; Li, H.; Chen, Q.; Steigerwald, M. L.; Venkataraman, L.; Nuckolls, C. *Chem. Sci.* **2014**, *5*, 1561.
(20) Su, T. A.; Widawsky, J. R.; Li, H.; Klausen, R. S.; Leighton, J. L.; Steigerwald, M. L.; Venkataraman, L.; Nuckolls, C. *J. Am. Chem. Soc.* **2013**, *135*, 18331.
(21) The calculated Ar−α bond length is essentially the same regardless of β in the molecules studied here. DFT optimizations

performed with a B3LYP functional and a 6-31G** basis set for light atoms or an LACVP** basis set for heavy atoms.

(22) Miller, T. M. In *CRC Handbook of Chemistry and Physics*, 96th ed.; Haynes, W. M., Ed.; CRC Press: Boca Raton, FL, 2015; pp 187–196.

(23) Allen, L. C. *J. Am. Chem. Soc.* **1989**, *111*, 9003.

(24) *Jaguar*, version 8.3; Schrodinger, Inc.: New York, NY, 2014.

(25) Quek, S. Y.; Khoo, K. H. *Acc. Chem. Res.* **2014**, *47*, 3250.

(26) Leary, E.; La Rosa, A.; González, M. T.; Rubio-Bollinger, G.; Agraït, N.; Martín, N. *Chem. Soc. Rev.* **2015**, *44*, 920.

(27) Su, T. A.; Neupane, M.; Steigerwald, M. L.; Venkataraman, L.; Nuckolls, C. *Nat. Rev. Mater.* **2016**, *1*, 16002.

(28) Whitmore, F. C.; Sommer, L. H. *J. Am. Chem. Soc.* **1946**, *68*, 481.

(29) Sommer, L. H.; Whitmore, F. C. *J. Am. Chem. Soc.* **1946**, *68*, 485.

(30) It is worth comparing the HOMO energy (B3LYP/cc-pVTZ) of **SiCSi** (−5.74 eV) with 4-methylthioanisole (−5.64 eV) because it demonstrates that C−H bonds energetically destabilize the thioanisole even more so than Si−C bonds do. The weaker interaction between π orbitals and Si−C bonds relative to C−H bonds is a common feature of the α silicon effect.

(31) Lambert, J. B. *Tetrahedron* **1990**, *46*, 2677.

(32) Hammett, L. P. *J. Am. Chem. Soc.* **1937**, *59*, 96.

(33) Venkataraman, L.; Park, Y. S.; Whalley, A. C.; Nuckolls, C.; Hybertsen, M. S.; Steigerwald, M. L. *Nano Lett.* **2007**, *7*, 502.

(34) Egorochkin, A. N.; Razuvaev, G. A.; Lopatin, M. A. *J. Organomet. Chem.* **1988**, *344*, 49.